

TRACING STELLAR WIND VARIABILITY FROM SPACE

J. Krtička¹ and A. Feldmeier²

Abstract. Mass-loss by winds constitute one of the crucial processes that determine the evolution and fate of stars. The amount of mass lost by a star per unit of time (the mass-loss rate) and its dependence on stellar parameters is therefore one of the crucial ingredients of any stellar evolutionary model. Being derived either from observation or theory, wind mass-loss rates are highly uncertain, in many cases by a factor of a few. The uncertainty in a determination of the mass-loss rate is to a large extent connected with the variability of the wind. We discuss how the observation of stellar winds from space can help trace the wind’s variability and its origin, and how that knowledge can be used to derive more precise wind mass-loss rates.

Keywords: Stars: winds, outflows, mass-loss, early-type, variables, hydrodynamics

1 Introduction

Stars lose mass during their evolution, and there are many different ways in which single stars do so. In general they can be divided into explosive events (e.g., supernovæ and LBV-type eruptions) and quasi-stationary outflows (winds and disks). The outflowing disks are discussed elsewhere within these proceedings (Baade, Carciofi & Labadie-Bartz, Sigut, and Kee [PAGE]). This contribution discussed the variability of three main types of stellar winds: line-driven winds of hot luminous stars, dust-driven winds from AGB stars, and coronal winds from cool stars.

Mass loss by winds has important consequences for different fields of astrophysics. Winds affect stellar evolution (De Loore et al. 1977; Maeder 1981), contribute to the mass and momentum input into the interstellar medium, and redistribute heavier elements created during stellar nucleosynthesis. Furthermore, the interaction zone between a wind and the interstellar medium is an important source of galactic cosmic-ray particles (Aharonian et al. 2019).

Stellar winds may be studied from different aspects, but the “holy grail” of wind studies is to understand how the wind *mass-loss rate* (amount of mass lost per unit of time) varies as a function of stellar parameters:

$$\dot{M} = \dot{M}(L, T_{\text{eff}}, M, Z, \dots) \quad [M_{\odot} \text{ yr}^{-1}]. \quad (1.1)$$

Although other wind parameters (for example, wind terminal velocity, wind angular momentum loss or wind X-ray emission) are important for specific issues, the wind mass-loss rate is indisputably the most important one. Despite significant efforts of many astronomers over last few decades, the wind mass-loss rates are not known with a precision sufficient for many applications. Below we discuss why that is the case, and how observations of wind variability can improve the situation.

2 Hot-star winds

Winds from hot stars are mostly driven by the light absorption (scattering) in the lines of “heavy” elements such as carbon, nitrogen, oxygen, silicon and iron (Castor et al. 1975). This type of stellar wind, which is propelled by stellar radiation, can be found in hot stars in various evolutionary phases, including main-sequence stars, OBA supergiants, hot subdwarfs, central stars of planetary nebulae and Wolf-Rayet stars. Although theoretical predictions of mass-loss rates exist for all these stellar types (e.g., Vink et al. 2001; Krtička & Kubát 2017), they differ from one another by factor of a few, and they also differ significantly from observational estimates.

¹ Masaryk University, Brno, Czech Republic

² Potsdam University, Potsdam-Golm, Germany

2.1 Hot-star wind mass-loss rate estimates and the influence of clumping

There are several methods that enable us to derive wind mass-loss rates from observations. However, there is no direct way of estimating those rates. Every method uses models or physical assumptions that enable us to quantify the amount of mass loss. As a result, significant discrepancies may exist between individual methods.

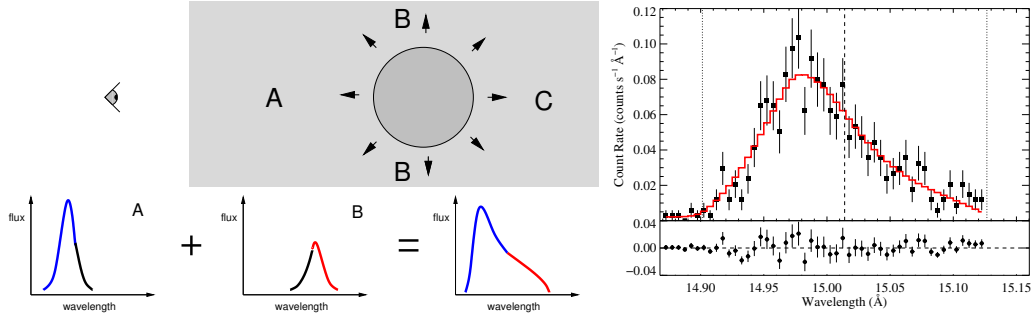


Fig. 1. X-ray line formation. **Left:** Lines originate from the whole wind volume, but the emission from part B is more absorbed on its way towards the observer than the emission from part A. **Right:** Observed profile (Leutenegger et al. 2013). © AAS. Reproduced with permission.

As a result of their supersonic nature, hot-star winds emit strong X-rays. Most X-rays are emitted by hot, shock-heated material at frequencies corresponding to individual line transitions. However, the bulk of the wind material is relatively cool and absorbs the X-rays in the continuum. Owing to the asymmetry of wind X-ray absorption (the X-rays emitted from the opposite hemisphere being more strongly absorbed than X-rays emitted in the hemisphere that faces the observer), the wind X-ray profiles become asymmetric (see Fig. 1). The level of asymmetry is a measure of the wind mass-loss rate (Owocki & Cohen 2001; Ignace & Gayley 2002).

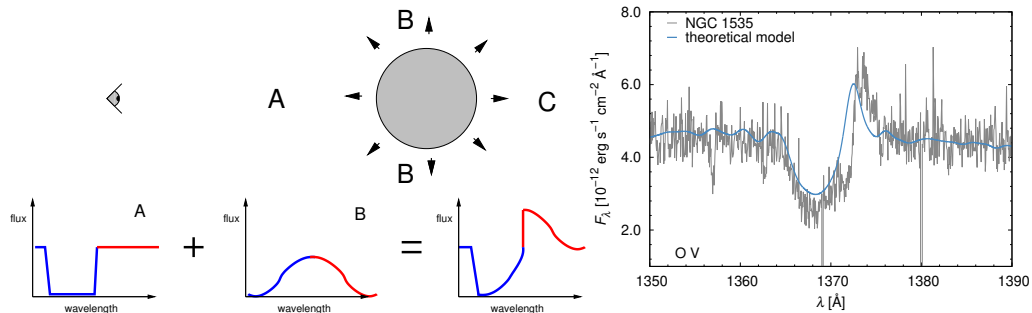


Fig. 2. Origin of P Cygni line profiles. **Left:** The P Cygni line profile is formed from an absorption component, which originates from intervening material in region A, and an emission component from material in regions A and B. Adopted from Owocki (2000). **Right:** Comparison of observed and theoretical P Cygni line profiles.

P Cygni and emission line profiles provide another mass-loss rate characteristic in the ultraviolet and optical domains. There, the strength of the emission-line components and the depth of unsaturated absorption components are proportional to the mass-loss rate (see Fig. 2).

Wind material causes a continuum excess that is especially strong in the infrared and radio domains (Fig. 3, Bieging et al. 1989; Scuderi et al. 1998). The amount of excess leads to another measure of the mass-loss rate.

The comparison of theoretical and observed mass-loss rate estimates in Fig. 4 (left) shows an order-of-magnitude discrepancy between individual values. From the point of view of observations, this discrepancy is probably caused by the influence of inhomogeneities (clumping) that may mimic higher mass-loss rates (in the case of optically thin clumps, e.g., Puls et al. 2006; Bouret et al. 2012) or decrease the absorption due to porosity effects in the case of optically thick clumps (Oskinova et al. 2007; Sundqvist et al. 2010; Šurlan et al. 2013).

The level of the influence which clumping can have upon observed characteristics is unclear. However, inhomogeneities also cause wind variability. The study of the wind variability using different wind observables may therefore help to constrain the structure of inhomogeneities and their influence on the mass-loss rate indicators.

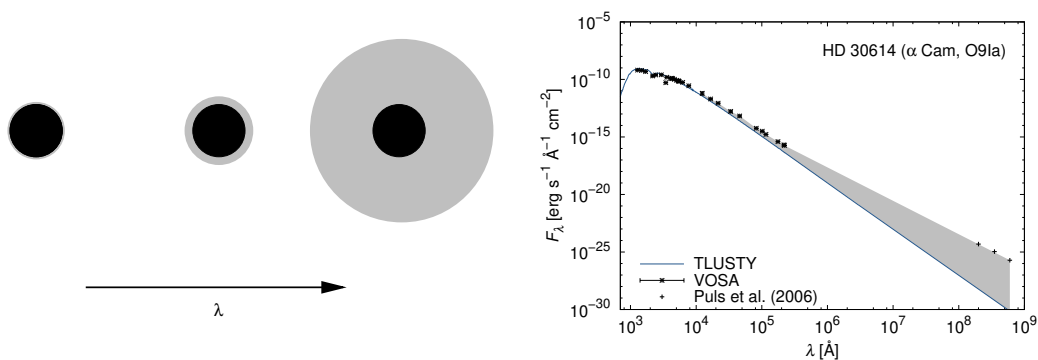


Fig. 3. Infrared and radio excess due to a stellar wind. **Left:** The radius of the optically thick region increases with increasing wavelength (adopted from Lamers & Cassinelli 1999). **Right:** Observed spectral energy distribution (VOSA and Puls et al. 2006) compared to the radiative flux from hydrostatic model atmospheres (Lanz & Hubeny 2007).

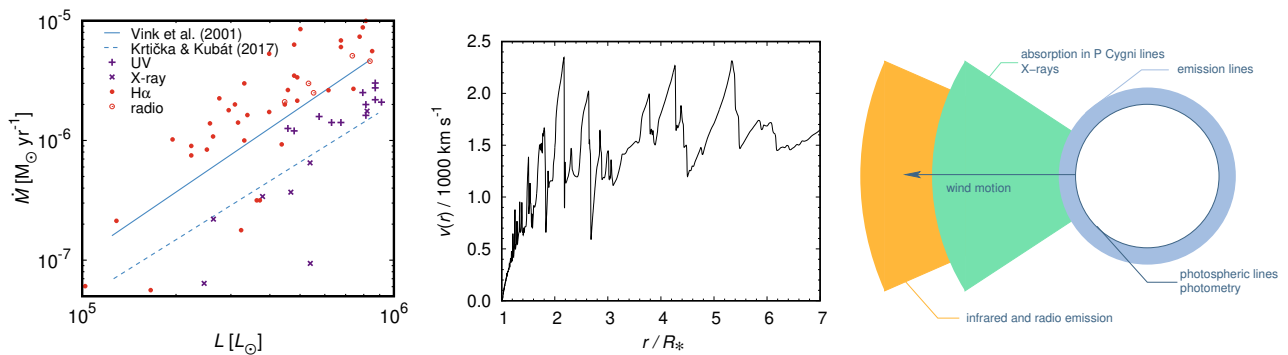


Fig. 4. **Left:** Comparison of theoretical (Vink et al. 2001; Krtićka & Kubát 2017) and observed (Scuderi et al. 1998; Mokieim et al. 2007; Bouret et al. 2012; Šurlan et al. 2013; Cohen et al. 2014) mass-loss rate determinations of O stars. **Middle:** A snapshot of simulations of hydrodynamical wind instability by Feldmeier et al. (1997), showing a radial dependence of velocity. **Right:** Origin of different observables in the winds of hot stars.

Different observables originate at different locations in the wind (Fig. 4, right). While optical photometry relates to the stellar atmosphere and at the wind base, $H\alpha$ emission comes from wind regions relatively close to the star. The X-ray emission and the absorption part of the P Cygni line profiles trace the supersonic part of the wind, up to the speed equal to its terminal velocity. The infrared and radio emission originate in an extended envelope at large distances from the star. Different origins of wind observables enables us to trace the wind structure from its possible origin at the stellar surface, through the development of strong inhomogeneities in the supersonic part of the wind, and up to the free movement of those clumps at large distances from the star.

2.2 Large scale wind structure: corotating interacting regions

Large-scale wind structure is the easiest to study. Its appearance is manifested as deep additional absorption components moving in blue parts of P Cygni line profiles (discrete absorption components, DACs, Fig. 5). The speed of the DACs, as inferred from their slope in the time *versus* Doppler-shift diagram (Fig. 5, right), is lower than the speed of the wind. A possible interpretation is that the evolution of DACs is the result of a projection effect of dense streams (corotating interacting regions) spiralling in the wind through stellar rotation (Fig. 5).

There are several effects that can test this model of corotating interacting regions. Overdensity implies a stronger radiative force across a small portion of the stellar surface. The radiative force can most easily be modulated by bright surface spots, which should in turn show up in the photometry. Indeed, many hot stars show periodic light variability with the same periods in which DACs appear. This was found from MOST observations of WR 110 (Chené et al. 2011) and ξ Per (O7.5 III(n)((f)), Ramaramanantsoa et al. 2014), and from K2 photometry of ρ Leo (B1 Iab, Aerts et al. 2018). The agreement is not always perfect, as shown from

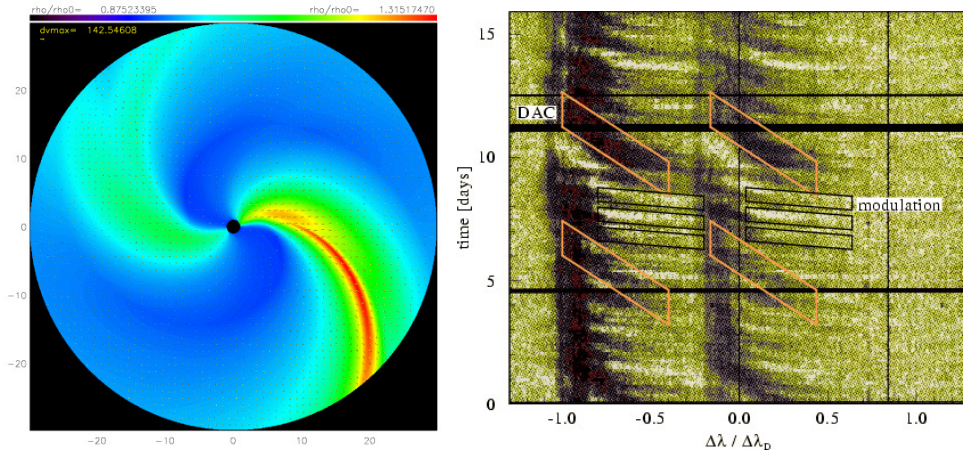


Fig. 5. Left: Origin of large-scale wind structure. Surface spots generate dense streams, which (owing to velocity plateaux and overdensities) lead to discrete absorption components (DACs, Cranmer & Owocki 1996; Lobel & Blomme 2008). © AAS. Reproduced with permission. **Right:** Time development of P Cygni line profiles. The abscissa shows the wavelength (or wind velocity); the ordinate shows time. Individual horizontal slices correspond to stellar spectra taken at different times with colour coded absorption. Deep, slowly moving absorption components (DACs) are superimposed on weak structures. The graph shows a doublet, so the structure consequently repeats at two different wavelengths. Credit: Hamann et al. (2001), reproduced with permission © ESO.

SMEI and BRITE observations of ζ Pup (O4I(n)fp, Howarth & Stevens 2014; Ramiaramanantsoa et al. 2018). On the other hand, the fact that theoretical models show that the detected level of light variability is able to account for the observed strength of DACs (David-Uraz et al. 2017) does support the model of corotating interacting regions.

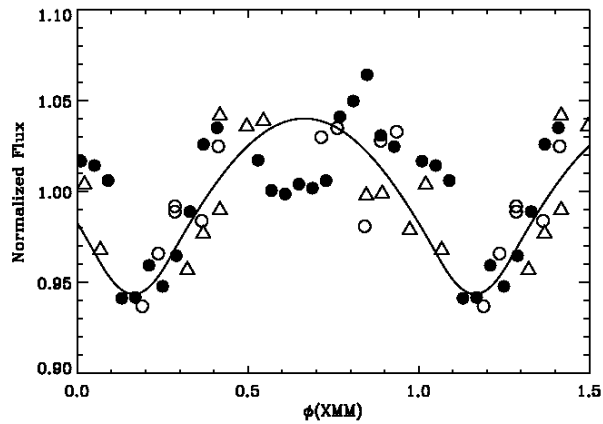


Fig. 6. O7.5 III(n)((f)) star ξ Per: X-ray flux (filled symbols) compared with UV data (open symbols). CIR variability of UV lines, $H\alpha$ emission, and X-ray flux are modulated with the same period (de Jong et al. 2001; Massa et al. 2019). © AAS. Reproduced with permission.

As the overdensities connected with corotating interacting regions move through the wind, they also affect other observable characteristics. They become visible in $H\alpha$ first (see Fig. 4 right), followed by the appearance as DACs (Kaper et al. 1997). The modulation of X-ray emission at the same period as that of DACs nicely completes the picture (Massa et al. 2019, Fig. 6).

2.3 Small scale wind structure: the effect of clumping

While the large-scale wind structure causes the most prominent observational effects, the small-scale structure has very important consequences for the mass-loss rate determination. The inhomogeneities due to the small-

scale wind structure influence significantly the wind observables, and are likely to cause the disagreement between theory and observations (Fig. 4, left). However, while the model of corotating interacting regions provides a consistent picture of large-scale wind structure, the model of small-scale wind structure does not seem to be so successful.

The small-scale wind structure (clumping) is probably caused by line-driven wind instability (Fig. 4, middle, Lucy & Solomon 1970; Owocki et al. 1988; Feldmeier & Thomas 2017), which either amplifies the photospheric perturbations seeded by subsurface turbulent motions (Feldmeier et al. 1997), or is self-initiated in the wind (Sundqvist et al. 2018). The aim of observational studies of wind clumping is to trace the inhomogeneities as they originate in the photosphere (or close to it) and develop in the wind, influencing different observables.

Multiple wind observations point to the existence of a small-scale stochastic wind structure. Very precise photometry from satellites like *Kepler*, *CoRoT* and *BRITE* show stochastic low-amplitude light variations in O stars (e.g., Blomme et al. 2011; Briquet et al. 2011; Aerts et al. 2017). The variations are attributed to sub-surface convection and to stellar oscillations, but part may also originate through wind blanketing and the line-driven wind instability, which had already developed in the stellar photosphere (Krtička & Feldmeier 2018) if the base perturbation is large enough. The surface velocity fields are expected to cause not only photometric variability but also photospheric line-profile variability. Aerts et al. (2017) indeed found similar frequencies in photometric and spectroscopic observations, but without a strong correlation.

As the perturbations propagate into the wind, they affect wind-line profiles. The effect of inhomogeneities (clumping) most likely leads to discordances in individual mass-loss rate determinations (Fig. 4, left). However, time-resolved observations do not show any obvious link between photospheric and wind variability from optical lines (Martins et al. 2015). It may be difficult to trace individual inhomogeneities, owing to their small masses, but this result shows that more research is needed in order to understand the connection between surface perturbations and wind inhomogeneities.

In a supersonic wind the instabilities steepen into shocks and cause X-ray emission (Owocki et al. 1988; Feldmeier et al. 1997, middle panel of Fig. 4). As a result of the stochastic nature of instabilities, one should expect some X-ray variability. However, such variability is not observed, implying that a large number of independent shocks contribute to the X-ray emission (Nazé et al. 2013).

3 Dust-driven winds of luminous cool stars

The acceleration of dust-driven winds of luminous cool stars is the result of a three-step process (Gilman 1972; Bowen 1988; Woitke 2006; Höfner & Olofsson 2018). Stellar pulsations cause large amounts of stellar material to be transported outwards and deposited at distances where the dust particles can condensate. The radiation then takes over and accelerates the wind by radiative forces on the dust particles. The bulk of the wind that is composed of hydrogen and helium is accelerated by collisions with dust particles.

Stellar variability is therefore a prerequisite for the formation of the wind. As the pulsation period is related to the stellar luminosity, one can expect some relation between the mass-loss rate and the pulsation period (or luminosity). This was indeed found for different types of AGB stars by Uttenthaler (2013).

4 Coronal winds of cool main-sequence stars

Cool solar-type stars have coronal winds through thermal expansion of the stellar corona (Parker 1958). While the mechanism of the coronal heating is still somewhat unclear (see Sakaue, [PAGE], for a recent model), it is clear that the heating process is closely related to stellar activity. For example, it explains the relation between time-series of the Ca II *H* and *K* lines and *ROSAT* X-ray fluxes (Hempelmann et al. 2003).

Mass-loss due to a *magnetized* stellar wind causes magnetic rotational braking (Weber & Davis 1967; Skumanich 1972; Kawaler 1988). With proper calibration, this can be used to estimate stellar ages from photometric periods (Angus et al. 2015).

5 Conclusions

Every estimate of a wind mass-loss rate is relatively uncertain. To a large extent, it is connected to small-scale wind structure, which leads to wind variability. We have shown here how wind variability can be used as a tracer of wind structure, so the study of wind *variability* can therefore improve our knowledge of the wind *structure*, leading to more reliable estimates of wind mass-loss rates.

JK was supported by grant GA ĀR 18-05665S.

References

- Aerts, C., Bowman, D. M., Sımon-Dıaz, S., et al. 2018, *MNRAS*, 476, 1234
- Aerts, C., Sımon-Dıaz, S., Bloemen, S., et al. 2017, *A&A*, 602, A32
- Aharonian, F., Yang, R., & de Ona Wilhelmi, E. 2019, *Nature Astronomy*, 3, 561
- Angus, R., Aigrain, S., Foreman-Mackey, D., & McQuillan, A. 2015, *MNRAS*, 450, 1787
- Biegging, J. H., Abbott, D. C., & Churchwell, E. B. 1989, *ApJ*, 340, 518
- Blomme, R., Mahy, L., Catala, C., et al. 2011, *A&A*, 533, A4
- Bouret, J.-C., Hillier, D. J., Lanz, T., & Fullerton, A. W. 2012, *A&A*, 544, A67
- Bowen, G. H. 1988, *ApJ*, 329, 299
- Briquet, M., Aerts, C., Baglin, A., et al. 2011, *A&A*, 527, A112
- Castor, J. I., Abbott, D. C., & Klein, R. I. 1975, *ApJ*, 195, 157
- Chene, A. N., Moffat, A. F. J., Cameron, C., et al. 2011, *ApJ*, 735, 34
- Cohen, D. H., Wollman, E. E., Leutenegger, M. A., et al. 2014, *MNRAS*, 439, 908
- Cranmer, S. R. & Owocki, S. P. 1996, *ApJ*, 462, 469
- David-Uraz, A., Owocki, S. P., Wade, G. A., Sundqvist, J. O., & Kee, N. D. 2017, *MNRAS*, 470, 3672
- de Jong, J. A., Henrichs, H. F., Kaper, L., et al. 2001, *A&A*, 368, 601
- De Loore, C., De Greve, J. P., & Lamers, H. J. G. L. M. 1977, *A&A*, 61, 251
- Feldmeier, A., Puls, J., & Pauldrach, A. W. A. 1997, *A&A*, 322, 878
- Feldmeier, A. & Thomas, T. 2017, *MNRAS*, 469, 3102
- Gilman, R. C. 1972, *ApJ*, 178, 423
- Hamann, W. R., Brown, J. C., Feldmeier, A., & Oskinova, L. M. 2001, *A&A*, 378, 946
- Hempelmann, A., Schmitt, J. H. M. M., Baliunas, S. L., & Donahue, R. A. 2003, *A&A*, 406, L39
- Hofner, S. & Olofsson, H. 2018, *A&A Rev.*, 26, 1
- Howarth, I. D. & Stevens, I. R. 2014, *MNRAS*, 445, 2878
- Ignace, R. & Gayley, K. G. 2002, *ApJ*, 568, 954
- Kaper, L., Henrichs, H. F., Fullerton, A. W., et al. 1997, *A&A*, 327, 281
- Kawaler, S. D. 1988, *ApJ*, 333, 236
- Krticka, J. & Kubat, J. 2017, *A&A*, 606, A31
- Krticka, J. & Feldmeier, A. 2018, *A&A*, 617, A121
- Lamers, H. J. G. L. M. & Cassinelli, J. P. 1999, *Introduction to Stellar Winds* (Cambridge University Press, [adsurl = https://ui.adsabs.harvard.edu/abs/1999isw..book....L](https://ui.adsabs.harvard.edu/abs/1999isw..book....L), [adsnote = Provided by the SAO/NASA Astrophysics Data System](#))
- Lanz, T. & Hubeny, I. 2007, *ApJS*, 169, 83
- Leutenegger, M. A., Cohen, D. H., Sundqvist, J. O., & Owocki, S. P. 2013, *ApJ*, 770, 80
- Lobel, A. & Blomme, R. 2008, *ApJ*, 678, 408
- Lucy, L. B. & Solomon, P. M. 1970, *ApJ*, 159, 879
- Maeder, A. 1981, *A&A*, 99, 97
- Martins, F., Marcolino, W., Hillier, D. J., Donati, J. F., & Bouret, J. C. 2015, *A&A*, 574, A142
- Massa, D., Oskinova, L., Prinja, R., & Ignace, R. 2019, *ApJ*, 873, 81
- Mokiem, M. R., de Koter, A., Vink, J. S., et al. 2007, *A&A*, 473, 603
- Naze, Y., Oskinova, L. M., & Gosset, E. 2013, *ApJ*, 763, 143
- Oskinova, L. M., Hamann, W.-R., & Feldmeier, A. 2007, *A&A*, 476, 1331
- Owocki, S. 2000, *Radiatively Driven Stellar Winds from Hot Stars* (Bristol: Institute of Physics Publishing), 1887
- Owocki, S. P., Castor, J. I., & Rybicki, G. B. 1988, *ApJ*, 335, 914
- Owocki, S. P. & Cohen, D. H. 2001, *ApJ*, 559, 1108
- Parker, E. N. 1958, *ApJ*, 128, 664
- Puls, J., Markova, N., Scuderi, S., et al. 2006, *A&A*, 454, 625
- Ramiamananantsoa, T., Moffat, A. F. J., Chene, A.-N., et al. 2014, *MNRAS*, 441, 910
- Ramiamananantsoa, T., Moffat, A. F. J., Harmon, R., et al. 2018, *MNRAS*, 473, 5532
- Scuderi, S., Panagia, N., Stanghellini, C., Trigilio, C., & Umana, G. 1998, *A&A*, 332, 251
- Skumanich, A. 1972, *ApJ*, 171, 565

- Sundqvist, J. O., Owocki, S. P., & Puls, J. 2018, *A&A*, 611, A17
- Sundqvist, J. O., Puls, J., & Feldmeier, A. 2010, *A&A*, 510, A11
- Uttenthaler, S. 2013, *A&A*, 556, A38
- Šurlan, B., Hamann, W.-R., Aret, A., et al. 2013, *A&A*, 559, A130
- Vink, J. S., de Koter, A., & Lamers, H. J. G. L. M. 2001, *A&A*, 369, 574
- Weber, E. J. & Davis, Leverett, J. 1967, *ApJ*, 148, 217
- Woitke, P. 2006, *A&A*, 452, 537